NeuroImage 105 (2015) 486–492

Contents lists available at ScienceDirect

NeuroImage

journal homepage: www.elsevier.com/locate/ynimg

Validation of quantitative susceptibility mapping with Perls' iron staining for subcortical gray matter

Hongfu Sun [a], Andrew J. Walsh [a], R. Marc Lebel [a], Gregg Blevins [b], Ingrid Catz [b], Jian-Qiang Lu [c], Edward S. Johnson [c], Derek J. Emery [d], Kenneth G. Warren [b], Alan H. Wilman [a,*]

[a] Department of Biomedical Engineering, University of Alberta, Edmonton, Alberta, Canada, T6G 2V2
[b] Division of Neurology, Department of Medicine, University of Alberta, Edmonton, Alberta, Canada, T6G 2G3
[c] Department of Laboratory Medicine and Pathology, University of Alberta, Edmonton, Alberta, Canada, T6G 2B7
[d] Department of Radiology and Diagnostic Imaging, University of Alberta, Edmonton, Alberta, Canada, T6G 2B7

ARTICLE INFO

Article history:
Accepted 4 November 2014
Available online 8 November 2014

Keywords:
Quantitative susceptibility mapping
Postmortem imaging
Perls' iron stain
Brain iron
Subcortical gray matter
R2* mapping

ABSTRACT

Quantitative susceptibility mapping (QSM) measures bulk susceptibilities in the brain, which can arise from many sources. In iron-rich subcortical gray matter (GM), non-heme iron is a dominant susceptibility source. We evaluated the use of QSM for iron mapping in subcortical GM by direct comparison to tissue iron staining. We performed in situ or in vivo QSM at 4.7 T combined with Perls' ferric iron staining on the corresponding extracted subcortical GM regions. This histochemical process enabled examination of ferric iron in complete slices that could be related to susceptibility measurements. Correlation analyses were performed on an individual-by-individual basis and high linear correlations between susceptibility and Perls' iron stain were found for the three multiple sclerosis (MS) subjects studied ($R^2 = 0.75, 0.62, 0.86$). In addition, high linear correlations between susceptibility and transverse relaxation rate (R2*) were found ($R^2 = 0.88, 0.88, 0.87$) which matched in vivo healthy subjects ($R^2 = 0.87$). This work validates the accuracy of QSM for brain iron mapping and also confirms ferric iron as the dominant susceptibility source in subcortical GM, by demonstrating high linear correlation of QSM to Perls' ferric iron staining.

Introduction

Iron accumulation in subcortical gray matter (GM) may serve as an important biomarker of normal aging (Aquino et al., 2009; Cherubini et al., 2009; Hallgren and Sourander, 1958; Schenck and Zimmerman, 2004), and of neurological diseases including Alzheimer's disease, Parkinson's disease, Huntington's disease and multiple sclerosis (MS) (Berg and Youdim, 2006; Chen et al., 1993; Dexter et al., 1991; Khalil et al., 2011; LeVine, 1997; Williams et al., 2012). The mechanisms behind iron accumulation are not yet fully understood, although iron may accumulate through inflammatory and destructive processes (Stephenson et al., 2014), and may relate to the presence and extent of neurodegeneration. Measuring the state of brain iron metabolism may provide important information on aging and neurological diseases.

MRI provides a variety of contrast mechanisms that are sensitive to brain iron (Haacke et al., 2005) including transverse relaxation rates R2 and R2*, and susceptibility methods such as phase and susceptibility-weighted imaging. Previous studies in healthy subjects have shown that R2 and R2* increase in iron-rich brain regions and correlate strongly with iron concentration (Drayer et al., 1986; Gelman et al., 1999; Langkammer et al., 2010; Li et al., 2009; Peran et al., 2007; Thomas et al., 1993). While sensitive to iron, R2 and R2* may be affected by other sources such as macromolecular and water content changes (Mitsumori et al., 2012), which makes them not specific to brain iron. The introduction of phase imaging minimizes the influence of changes in macromolecular and water content, and is able to distinguish between negative and positive susceptibility sources (Duyn et al., 2007; Haacke et al., 2004; Rauscher et al., 2005). In addition, phase imaging has demonstrated good correlation to brain iron in subcortical GM (Haacke et al., 2007; Ogg et al., 1999; Yao et al., 2009). However, the non-local field properties of phase imaging cause it to be dependent on the shape and orientation of the object to the main magnetic field (Li and Leigh, 2004; Marques et al., 2009), which complicates interpretation.

The developing field of quantitative susceptibility mapping (QSM) inherits the iron sensitivity from phase imaging while eliminating the problem of non-locality. Derived from a deconvolution process from

Abbreviations: QSM, quantitative susceptibility mapping; EDSS, Expanded Disability Status Scale; PRELUDE, Phase Region Expanding Labeller for Unwrapping Discrete Estimates; SHARP, Sophisticated Harmonic Artifact Reduction for Phase data; RESHARP, Regularization Enabled SHARP; TV, total variation; GP, globus pallidus; PU, putamen; CN, caudate nucleus; RN, red nucleus; SN, substantia nigra; TH, thalamus.

* Corresponding author at: Department of Biomedical Engineering, University of Alberta, 1098 Research Transition Facility, Edmonton, Alberta, T6G 2V2, Canada.
E-mail address: wilman@ualberta.ca (A.H. Wilman).

http://dx.doi.org/10.1016/j.neuroimage.2014.11.010
1053-8119/

phase images, QSM unveils the local tissue susceptibility directly (de Rochefort et al., 2010; Kressler et al., 2010; Li et al., 2011; Liu et al., 2009, 2011; Reichenbach, 2012; Schweser et al., 2011; Shmueli et al., 2009; Wharton and Bowtell, 2010). A number of in vivo susceptibility maps have shown good correlations with subcortical GM iron concentrations (Bilgic et al., 2012; Schweser et al., 2011; Wu et al., 2012) as estimated from the hallmark study on brain iron by Hallgren and Sourander (1958). Nevertheless, validation of QSM for brain iron mapping requires postmortem studies that make a direct comparison between MRI and histochemistry. Only two human postmortem studies have been performed to date that compare QSM to histochemically measured iron content in subcortical GM. These studies used mass spectrometry (Langkammer et al., 2012) or X-ray emission and fluorescence (Zheng et al., 2013). The Langkammer et al. (2012) study provided absolute iron values but in small samples that do not provide a full spatial map of the tissue to relate to the susceptibility map, while the work by Zheng et al. (2013) used previously frozen formalin fixed tissue for MRI rather than in situ imaging. Furthermore, both studies examined total iron (ferrous and ferric). Thus to further validate QSM for subcortical GM iron mapping and to verify ferric iron as the main susceptibility source, there remains a need to compare in situ and in vivo susceptibility maps directly to spatial maps of ferric iron. In this study, we make use of Perls' iron staining (Meguro et al., 2007) to obtain full slice spatial maps of relative ferric iron content and compare to in situ and in vivo QSM in subcortical GM.

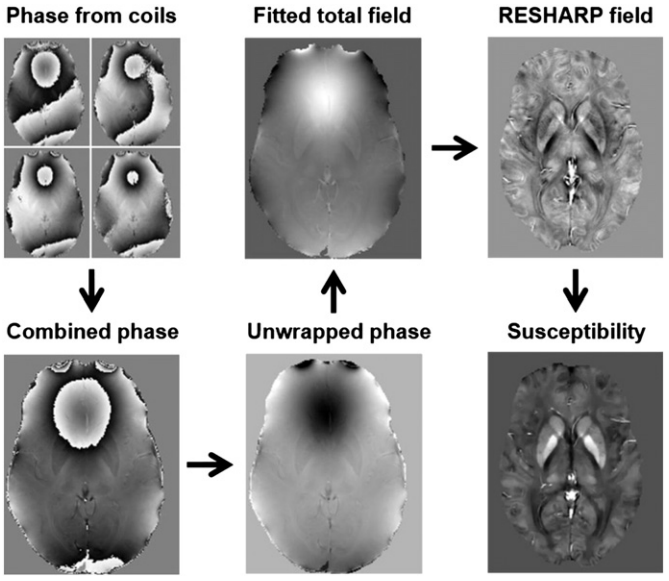

Fig. 1. The workflow for generating susceptibility maps from raw phase measurements. Phase-arrayed coils were combined after removing phase-offsets, and unwrapped using PRELUDE, then fitted to echo times. Background field was then removed using RESHARP, followed by susceptibility inversion using total variation regularization.

Material and methods

Subjects

In situ or in vivo QSM followed by Perls' iron staining was performed on three subjects who have been previously studied for phase, R2, and R2* mapping (Walsh et al., 2013). Subject 1 was a 63 year old male imaged in situ 28 h after death. Subject 2 was a 60 year old male imaged in situ 7 h after death. Subject 3 was a 45 year old male imaged in vivo one year before death. Subjects 1 and 2 had secondary progressive MS with Expanded Disability Status Scale (EDSS) scores of 8.5 before death, and disease durations of approximately 40 years. Subject 3 had relapsing remitting MS for 7 years with EDSS of 3.5 at time of imaging. Postmortem brains were fixed in formalin for 2 weeks, 6 months, and 6 weeks respectively before extraction for Perls' iron staining. The brain temperatures of postmortem Subject 1 and 2 were ~29 °C and 14 °C during MRI as estimated according to Al-Alousi et al. (2001). In addition, QSM and R2* were performed on three healthy male volunteers (age 48 ± 6 yrs). For all subjects, institutional ethical approval and informed consent from the subjects and/or their families were obtained.

MRI acquisition

Three-dimensional multiple gradient-echo acquisitions were collected at 4.7 T (Varian, Palo Alto, CA) either in situ or in vivo. Acquisition parameters were: field-of-view 256 × 128–160 × 160 mm; spatial resolution 1 × 0.8–1 × 2 mm; 80 axial slices; TR 44 ms; 10 echoes with echo spacing 4.1 ms; first echo time 2.9–3.2 ms; flip angle 10°; readout bandwidth 352 Hz/voxel; total acquisition time 8.9 min. A birdcage head coil was used for radiofrequency transmission and a tight-fitting 4-channel array coil for signal reception. The raw k-space datasets were saved and moved offline for image reconstruction.

Image reconstruction

Susceptibility maps were reconstructed from the raw phase images, following three main steps: phase pre-processing, background field artifact removal, and susceptibility inversion, as demonstrated in Fig. 1. In the phase pre-processing step, raw phase measures from the 4 independent receiver channels were combined after removing the receiver phase offsets estimated from the first two echoes as previously described (Robinson et al., 2011). The brain was extracted using the brain extraction tool (Smith, 2002) of FMRIB software library (FSL) on each echo. Aliased phase images were unwrapped in 3D with Phase Region Expanding Labeller for Unwrapping Discrete Estimates (PRELUDE) (Jenkinson, 2003) of FSL. A single field map was generated by linearly fitting the unwrapped phase maps to echo times, weighted by the masked magnitudes of each echo to increase the reliability of the fitting. Background field, mainly due to air-tissue susceptibility interfaces, was removed using RESHARP ("Regularization Enabled Sophisticated Harmonic Artifact Reduction for Phase data") (Sun and Wilman, 2013), which applies Tikhonov regularization on SHARP ("Sophisticated Harmonic Artifact Reduction for Phase data") (Schweser et al., 2011) to suppress non-harmonic artifacts from sources other than air-tissue susceptibility interfaces. The Tikhonov regularization parameter was set to 1×10^{-3} determined by the L-curve method. Finally, single-angle dipole inversion from local field to susceptibility was performed using the total variation (TV) regularization approach, which is the L1 norm of the gradients, and is similar to Bilgic et al. (2012), Liu et al. (2011), and Wu et al. (2012), with regularization parameter on the TV term selected as 5×10^{-4} by the L-curve method, after normalization to the main magnetic field in the unit of parts-per-million (ppm). In addition to susceptibility maps, R2* maps were also reconstructed as previously described (Lebel et al., 2012), using mono-exponential fit of all echoes, after a linear field gradient correction to compensate the air-tissue susceptibility dephasing effect.

Perls' iron staining and photographic processing

The brains of the subjects were removed at postmortem in accord with standard autopsy protocol, fixed in 18% formalin, and sectioned in 8 mm slices. Subject 1 was cut axially, while Subject 2 and 3 were cut in standard coronal sections. Slices containing subcortical GM were photographed and then stained with Perls' iron reagents (Meguro et al., 2007) by immersing in 1 L of 2% hydrochloric acid mixed with